

Supplementary Information

Heteroatoms driven activation and conversion of CO₂ using cyclophosphazene based inorganic-organic hybrid nanoporous materials

Ruchi Sharma^a, Raeesh Muhammad^a, Vimal Chandra Srivastava^b and Paritosh Mohanty^{a*}

^aFunctional Materials Laboratory, Department of Chemistry, IIT Roorkee, Roorkee-247667, Uttarakhand, India

^bDepartment of Chemical Engineering, IIT Roorkee, Roorkee-247667, Uttarakhand, India

*E-mail: paritosh75@gmail.com, pm@cy.iitr.ac.in

Experimental details

Materials

All the experiments were carried out using the as-supplied analytical grade reagents without purification. Phosphonitrilic chloride trimer (PNC, 99%, Sigma Aldrich), tetrahydrofuran (THF, SRL), melamine (Sigma-Aldrich), 4-hydroxybenzaldehyde (99%, Sigma Aldrich), dimethyl sulphoxide (DMSO, Fisher Scientific), hydrochloric acid (HCl, Merck), epichlorohydrin (SRL), epibromohydrin (Avra), styrene oxide (Alfa Aesar), glycidyl phenyl ether (Alfa Aesar), propylene oxide (Alfa Aesar) and 1,2-epoxyhexane (Alfa Aesar).

Synthesis of catalysts (HNM and CHNM)

The synthesis of HNM and CHNM have been carried out in two steps.^{1,2} In the first step, the precursor was synthesized by reacting PNC and 4-hydroxybenzaldehyde dissolved in THF under argon atmosphere for 48 h, at RT under stirring condition. The second step involves the condensation of precursor with melamine and pyrrole to produce HNM and CHNM, respectively.^{1,2} In a typical synthesis of HNM, 1:3 ratio of the precursor (1 mmol) and melamine (3 mmol) dissolved in 30 ml DMSO were refluxed for 48 h under N₂ atmosphere. An off-white product was collected after washing with methanol, THF followed by Soxhlet extraction with diethyl ether, and dried at 100 °C in hot air oven. A brown monolith of CHNM was synthesized at 180 °C for 48 h by a solvothermal treatment of 1 mmol of the precursor and 6 mmol of pyrrole (freshly distilled) dissolved in 5 ml 1,4-dioxane which was pre-treated for 1 h at 70 °C under N₂ atmosphere. The monolith was washed several times with methanol and THF and dried in vacuum at 80 °C. Structures of HNM and CHNM frameworks are shown in Fig.S1.

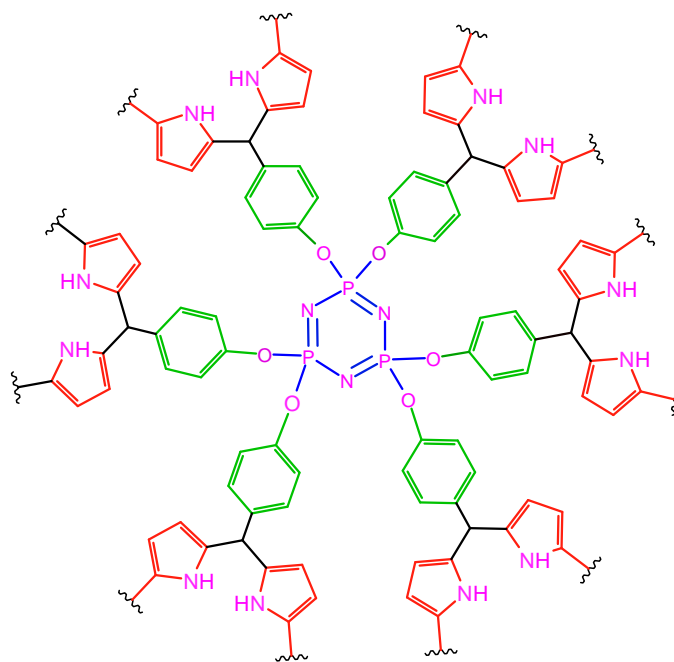
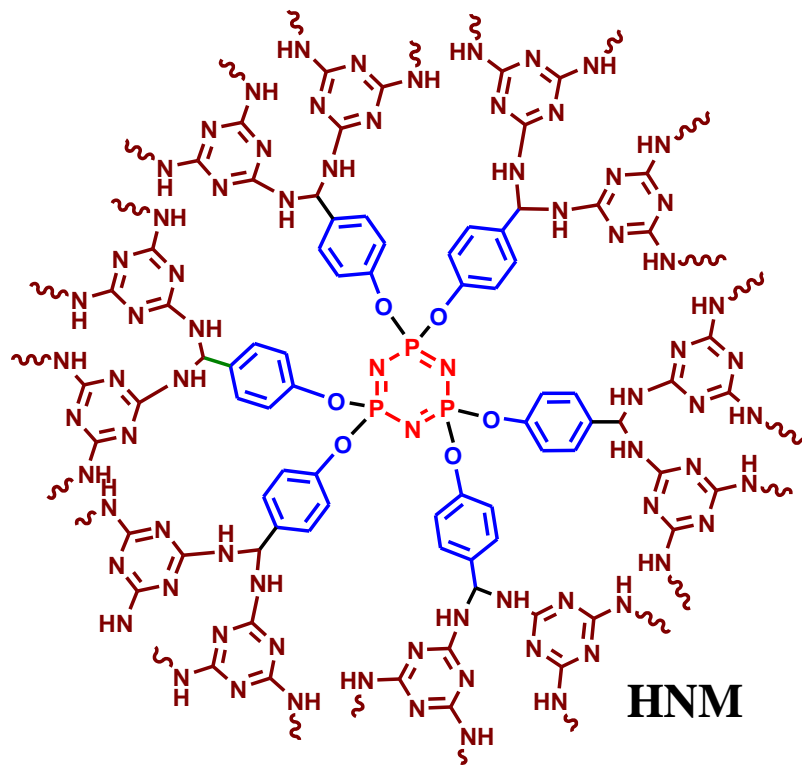
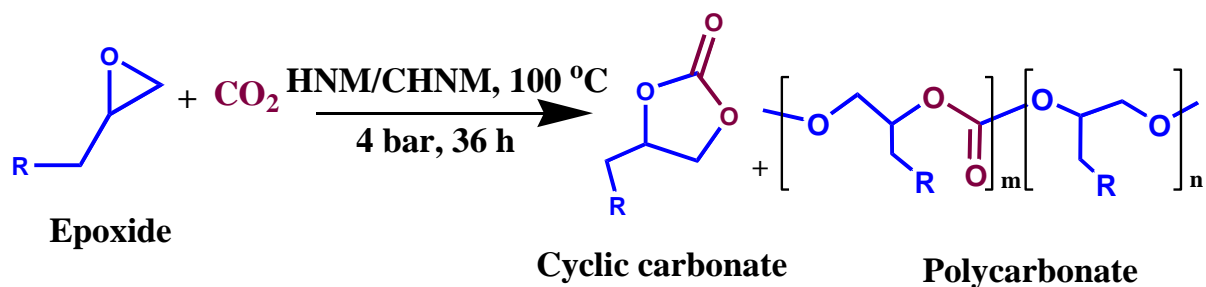


Fig. S1: Framework structure of HNM and CHNM.

Catalytic conversion of CO₂ into cyclic carbonates

As shown in scheme S1, in a typical synthesis, about 0.5 ml of the epoxide and 10 mg of the catalyst (either HNM or CHNM) was placed in a Teflon lined stainless-steel high-pressure reactor pressurized with 4 bar of CO₂. It was heated at 100 °C and the experiments were carried out for different time interval from 4 to 40 h. The reactor was allowed to cool naturally and the reaction mixture was diluted with ethyl acetate from which the catalyst was separated by centrifugation. The product was obtained by evaporating the solvent under reduced pressure. The obtained crude product was characterized by ¹H and ¹³C NMR spectroscopy.



Scheme S1: Conversion of CO₂ and epoxides to cyclic and polycarbonates using heteroatom enriched high surface area materials HNM and CHNM.

General characterization

The FT-IR spectra of the synthesized specimens HNM and CHNM were recorded using PerkinElmer Spectrum two FT-IR spectrophotometer with the wavelength range of 400-4000 cm^{-1} . Chemical environment and oxidation state of the elements in the specimens were investigated using XPS (X-ray Photoelectron spectrometer, PHI-5000 VersaProbe III, ULVAC-PHI INC) and spectra was recorded using Al $K\alpha$ as radiation source with analyzer pass energies of 280 eV for survey scan and 55 eV for high resolution scan of individual elements. The TGA/DTG analysis were carried out at the temperature range of 25-900 $^{\circ}\text{C}$ with heating rate of 10 $^{\circ}\text{C}/\text{min}$ under Ar atmosphere on EXSTAR TG/DTA 6300. The XRD pattern was recorded on Rigaku ultima IV in 2θ range of 5-80 $^{\circ}$ using Cu $K\alpha$ ($\lambda = 1.5405 \text{ \AA}$). The microstructure of the specimens investigated using FE-SEM (Carl Zeiss Gemini 300) and TEM (TECNAI G2S-TWIN). The Brunauer Emmett Teller specific surface area (S_{ABET}) were estimated using the standard N_2 sorption analysis in Autosorb iQ2, Quantachrome instruments, USA. Prior to the analysis, the sample was degassed at 120 $^{\circ}\text{C}$ for 6 h. The investigation of the products formed after cycloaddition of CO_2 to epoxides using HNM and CHNM as organocatalyst were carried out using liquid state ^1H and ^{13}C NMR using JEOL RESONANCE ECX-400.

Table S1: Assignment of FT-IR bands for CHNM and HNM.

Bands Assignment	Bands (cm ⁻¹)		
	Precursor	HNM	CHNM
N-H stretching	-	3405	3430
Aromatic –C–H stretch	3100	3105	3105
Aliphatic C–H stretching	-	2930	2930
Aldehydic C–H stretching	2840	-	-
–CHO stretching	1700	-	-
Pyrrole -C-N stretching	-	-	1690
C=C aromatic ring stretching	1585	1600	1600
Quadrant stretching of s-triazine ring	-	1548	-
Semicircle stretching of s-triazine ring	-	1477	-
Quadrant stretching of s-triazine ring	-	1548	-
Pyrrole ring stretching	-	-	1500
N-H bending	-	1650	1400
Ring and side chain CN stretching	-	1360	-
$\nu_{as}(P=N-P)$,	1210-1130	1210-1160	1210-1160
$\nu_{as}(P-O-C)$ vibration	980	986	960
ring deformation, (N-H, C2-H)	-	-	895
C-H out of plane wagging	793	850	760
C=C aromatic ring bending	680	814	685
$\delta(P=N-P)$ vibration	525	584	510

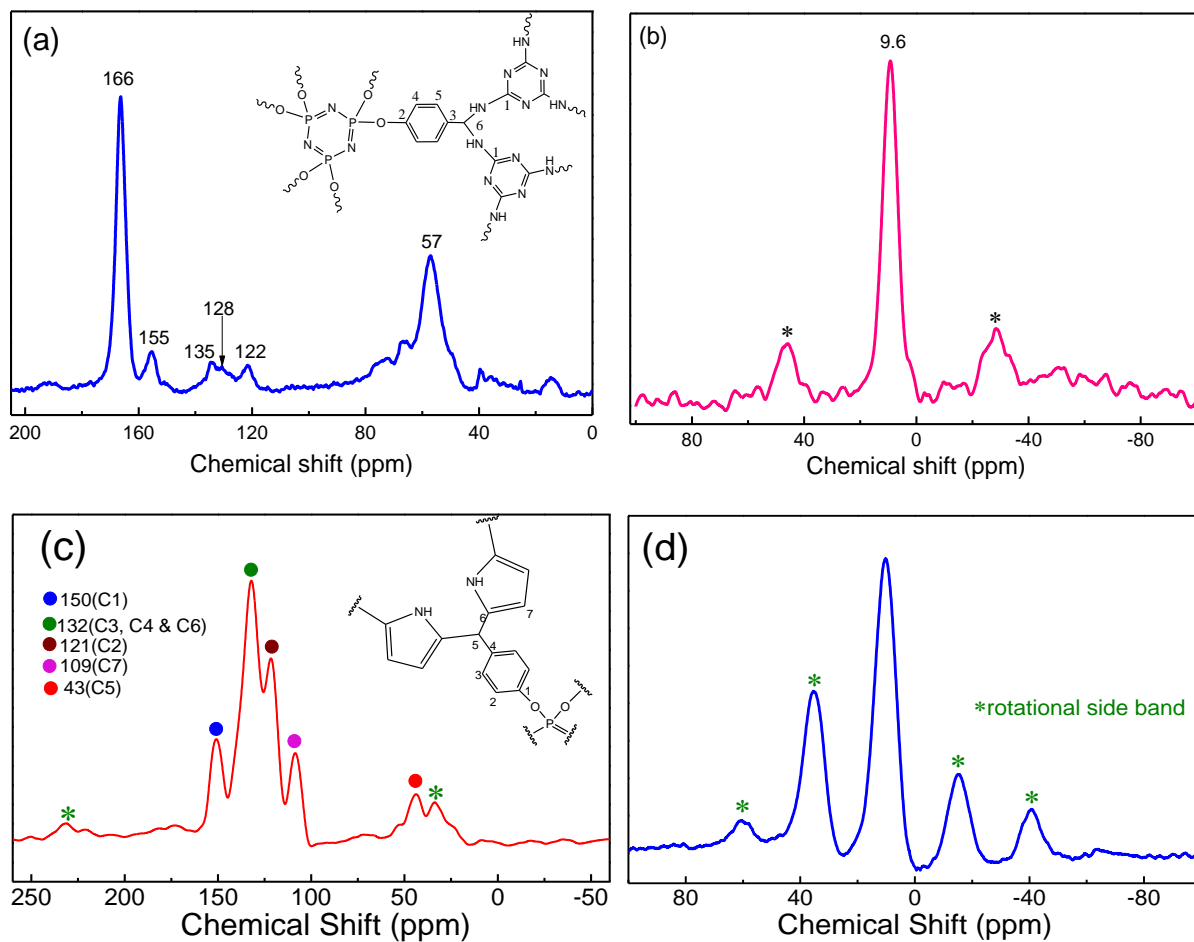


Fig. S2: (a), (c) ^{13}C CP-MAS NMR and (b), (d) ^{31}P CP-MAS NMR spectra of HNM and CHNM. The (*) are ascribed to rotational side bands. Reprinted with permission from ref. 9b. Copyright 2016, Royal Society of Chemistry. Reprinted with permission from ref. 9c. Copyright 2018, Elsevier.

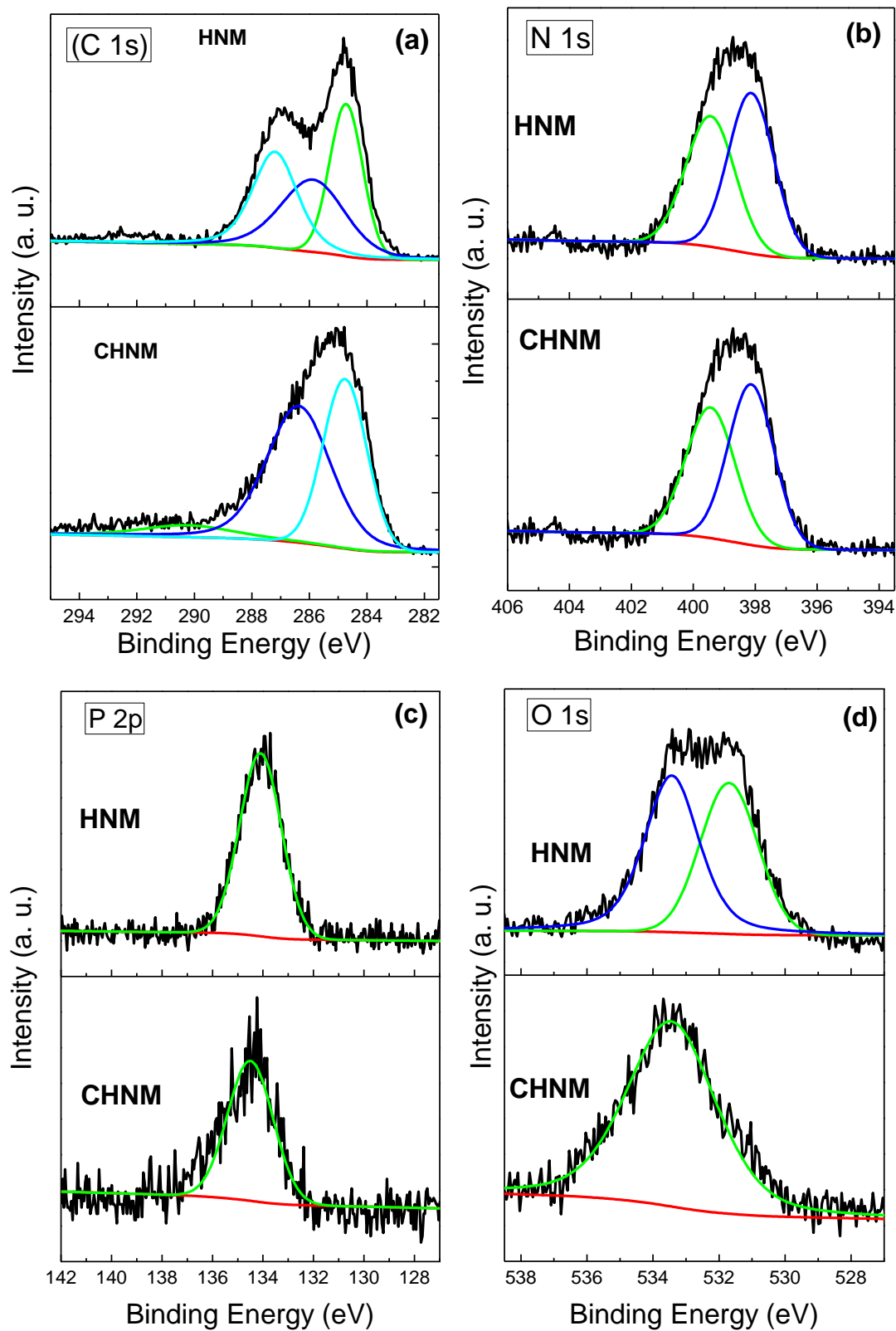


Fig. S3: XPS high resolution XPS spectra; (a) C 1s, (b) N 1s, (c) P 2p and (d) O 1s for CHNM and HNM.

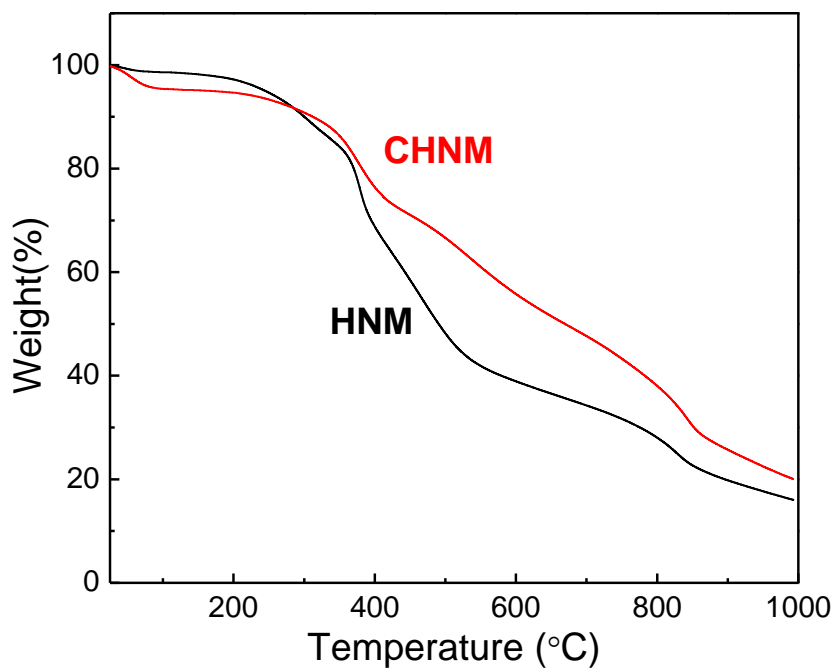


Fig. S4. TGA of HNM and CHNM measured in argon atmosphere.

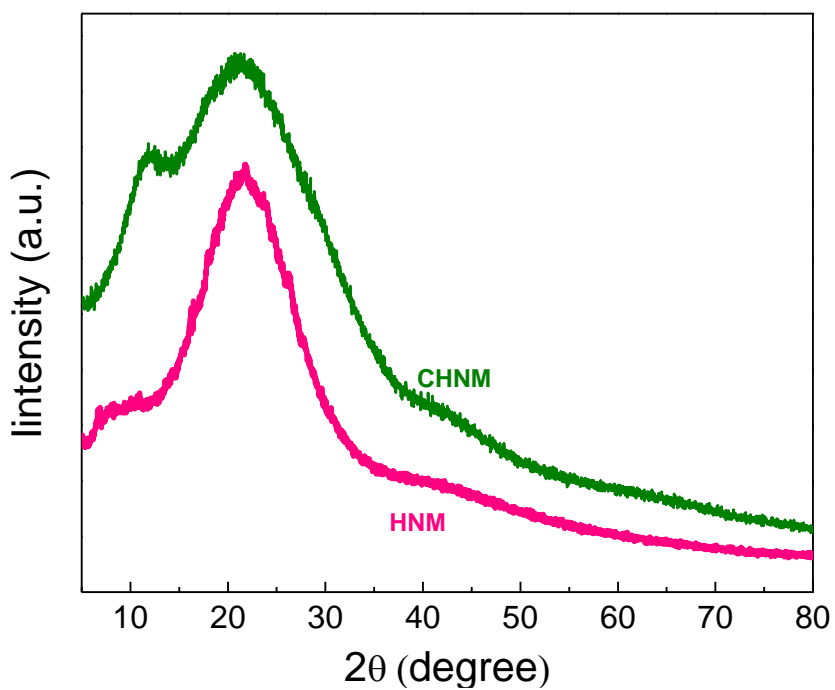


Fig. S5. X-ray diffraction patterns of HNM and CHNM.

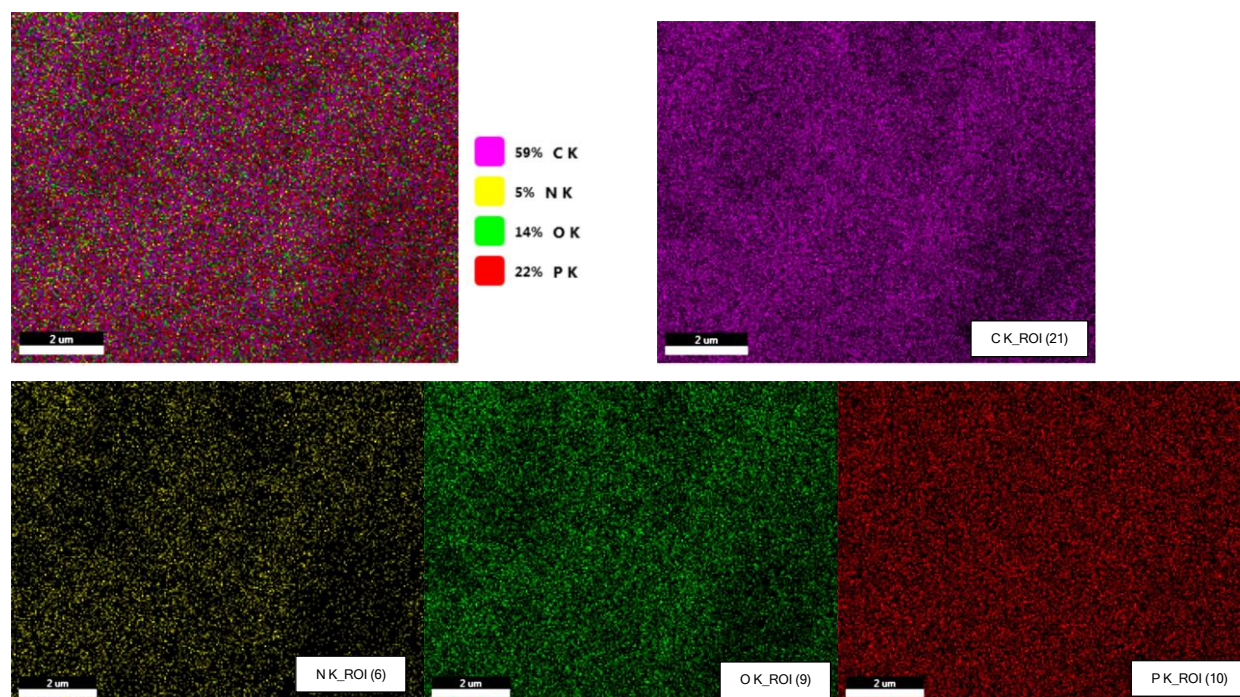


Fig. S6. EDAX mapping of elements C, N, O, and P in CHNM.

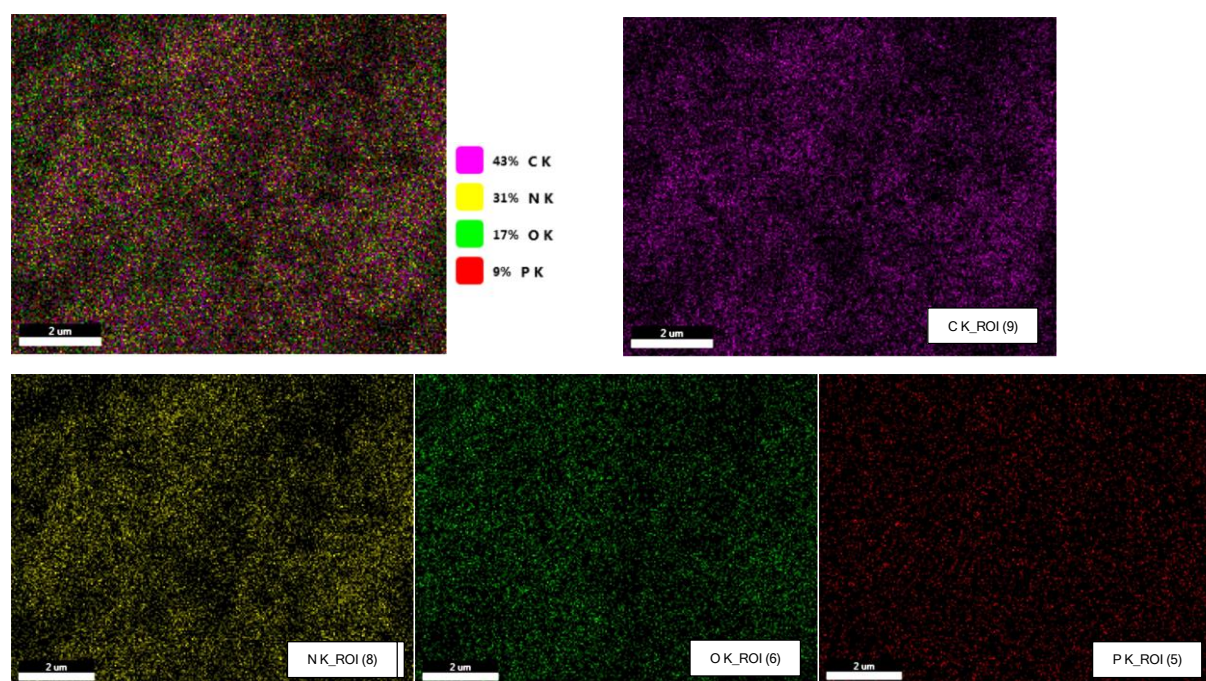


Fig. S7. EDAX mapping of elements C, N, O, and P in HNM.

Table S2: Reaction parameter optimization using epichlorohydrin as epoxide substrate.

S.No.	Catalyst HNM (mg)	Time (h)	Pressure (bar)	Conversion (%)
1.	20	36	4	100
2.	10	36	4	100
3.	5	36	4	51
8.	-	36	4	-
9.	10	36	2	44

Epoxide = 500 μ l; Temperature =100 $^{\circ}$ C.

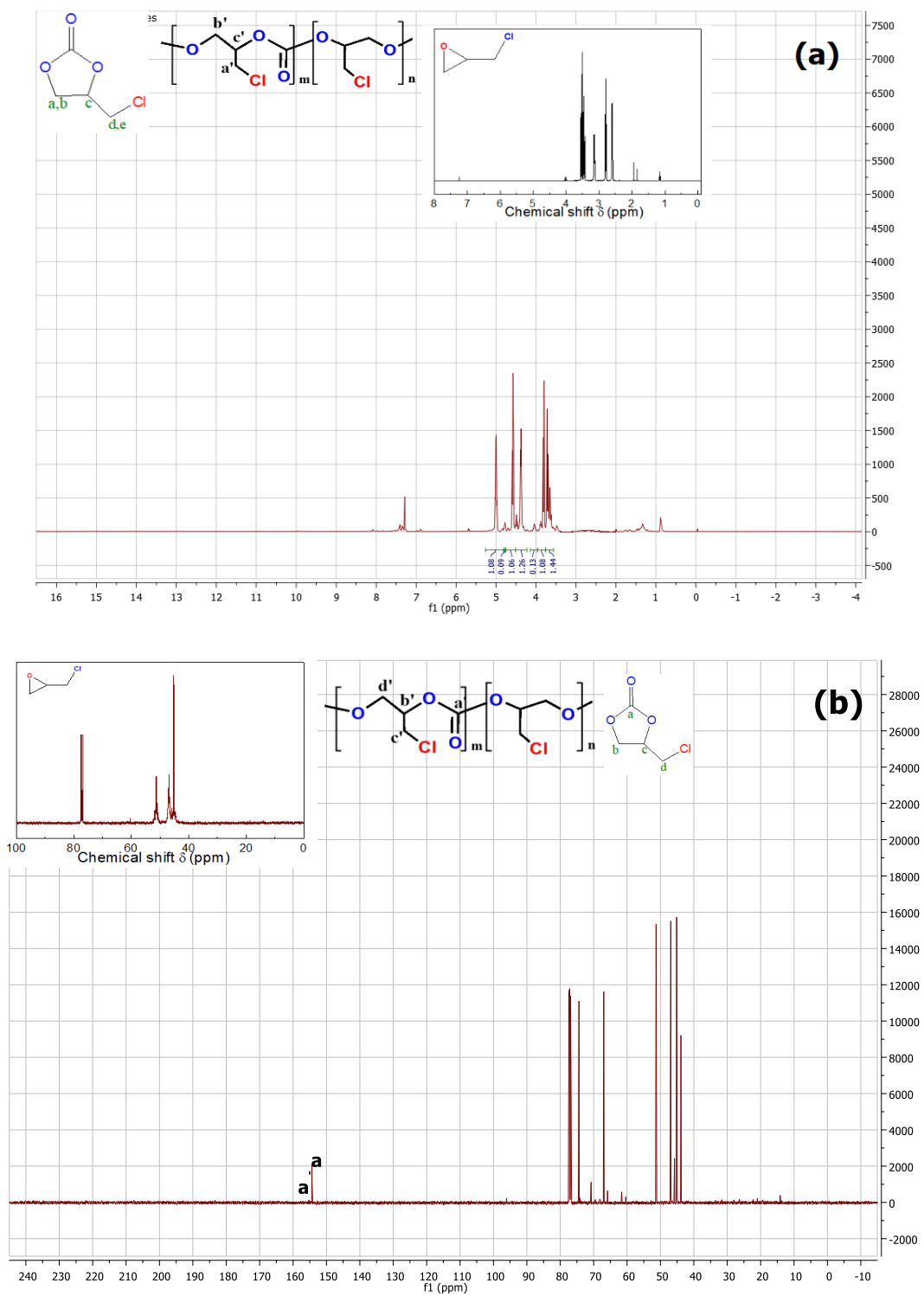


Fig. S8. (a) Crude ^1H NMR and (b) ^{13}C NMR spectrum of 4-chloromethyl-1,3-dioxolan-2-one catalyzed by HNM.

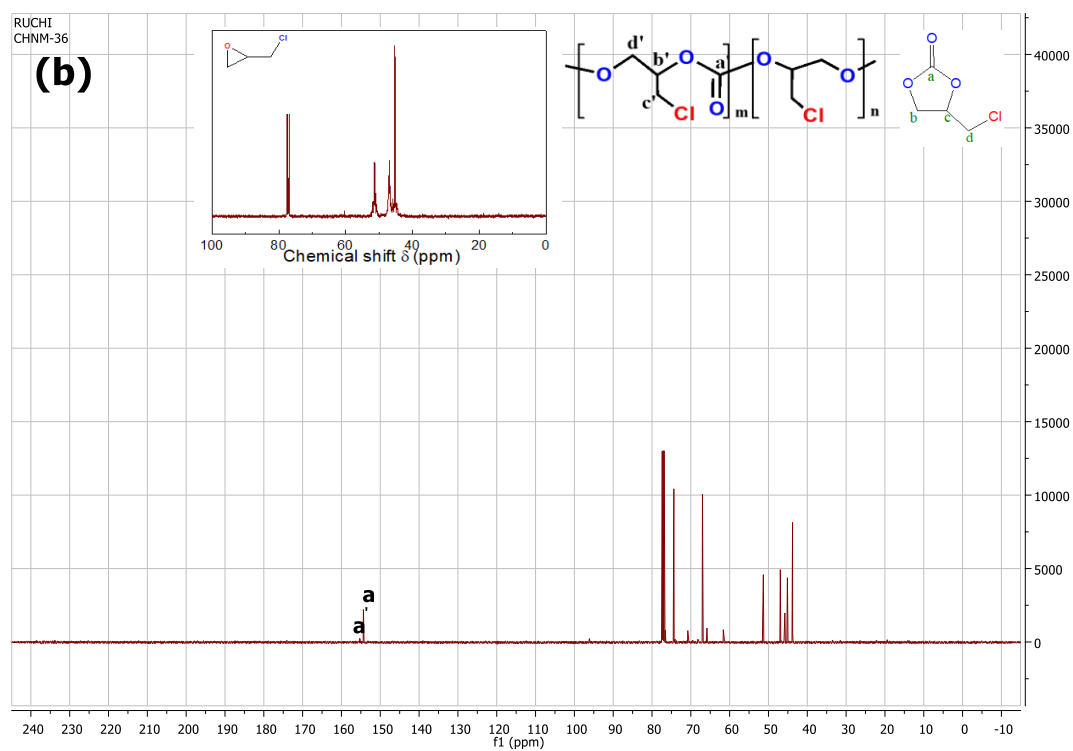
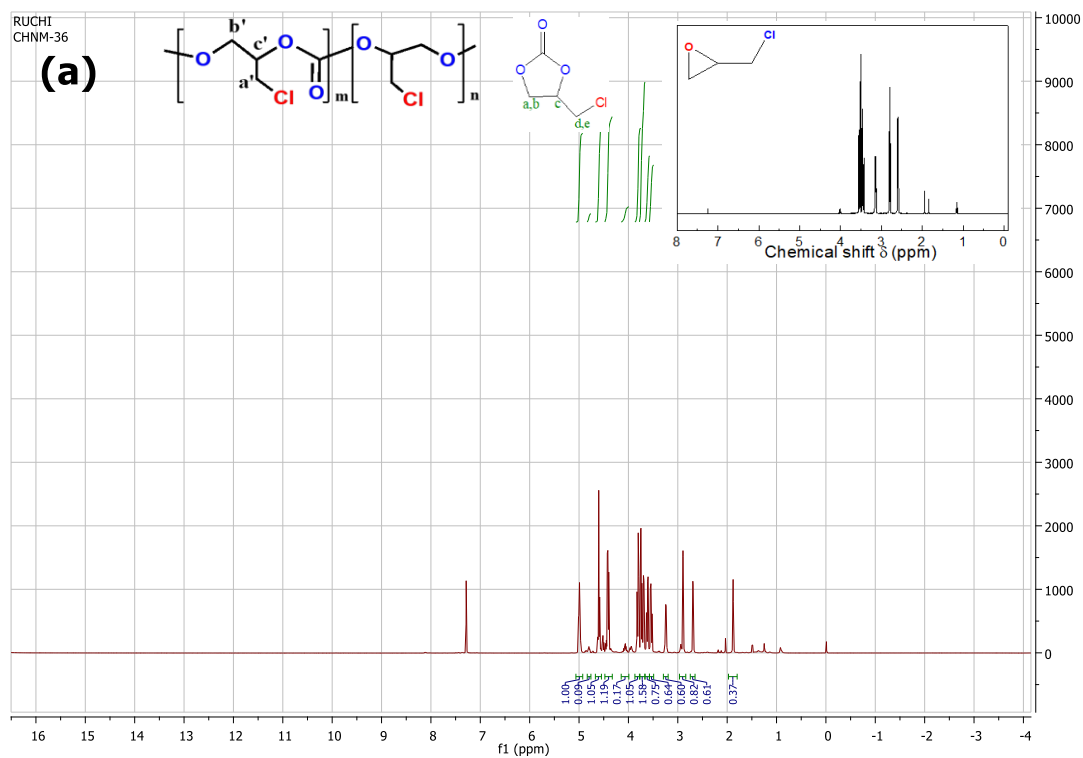


Fig. S9. (a) Crude ^1H NMR and (b) ^{13}C NMR spectrum of 4-chloromethyl-1,3-dioxolan-2-one catalyzed by CHNM.

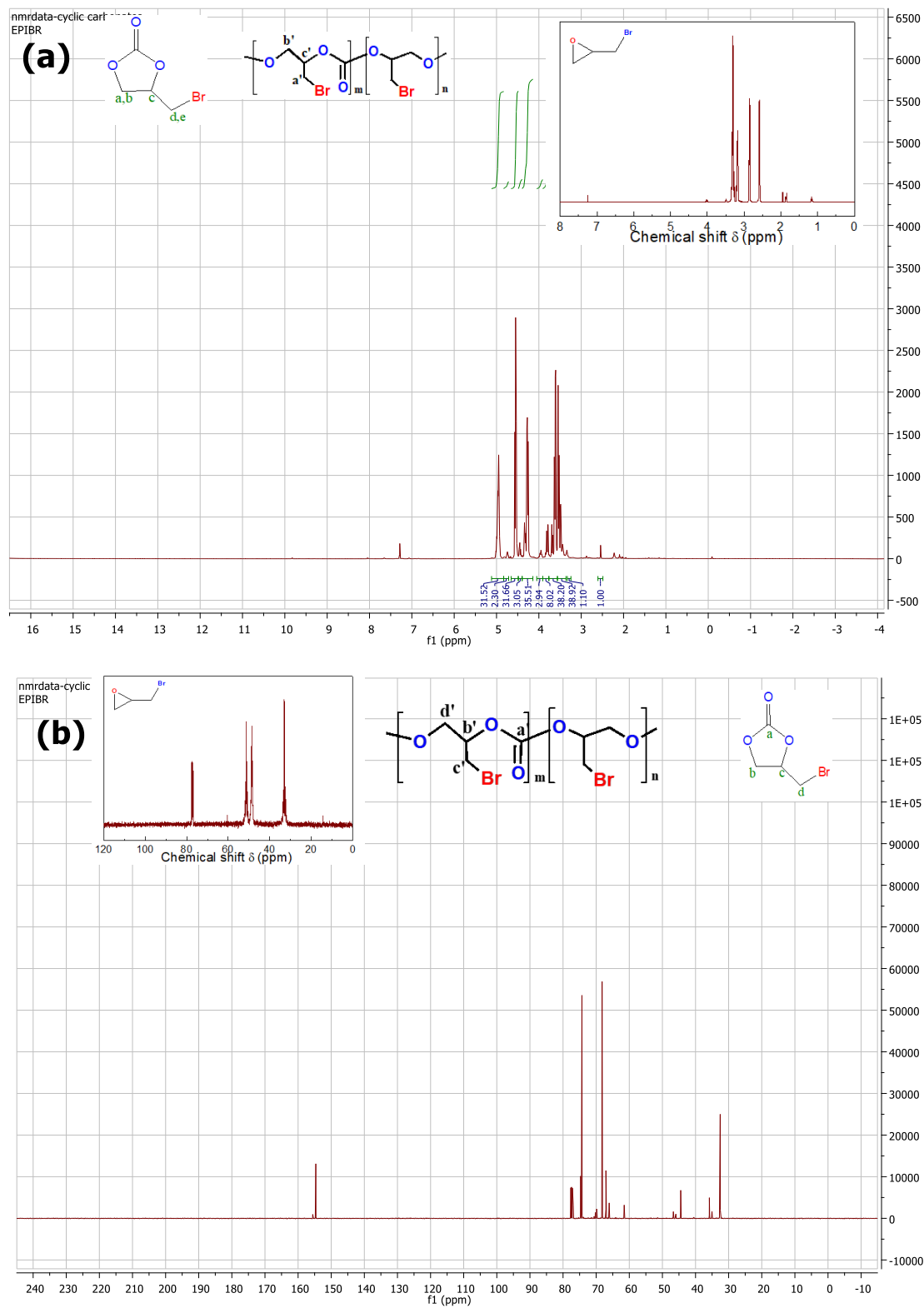


Fig. S10. (a) Crude ^1H NMR and (b) ^{13}C NMR spectrum of 4-bromomethyl-1,3-dioxolan-2-one catalysed by HNM.

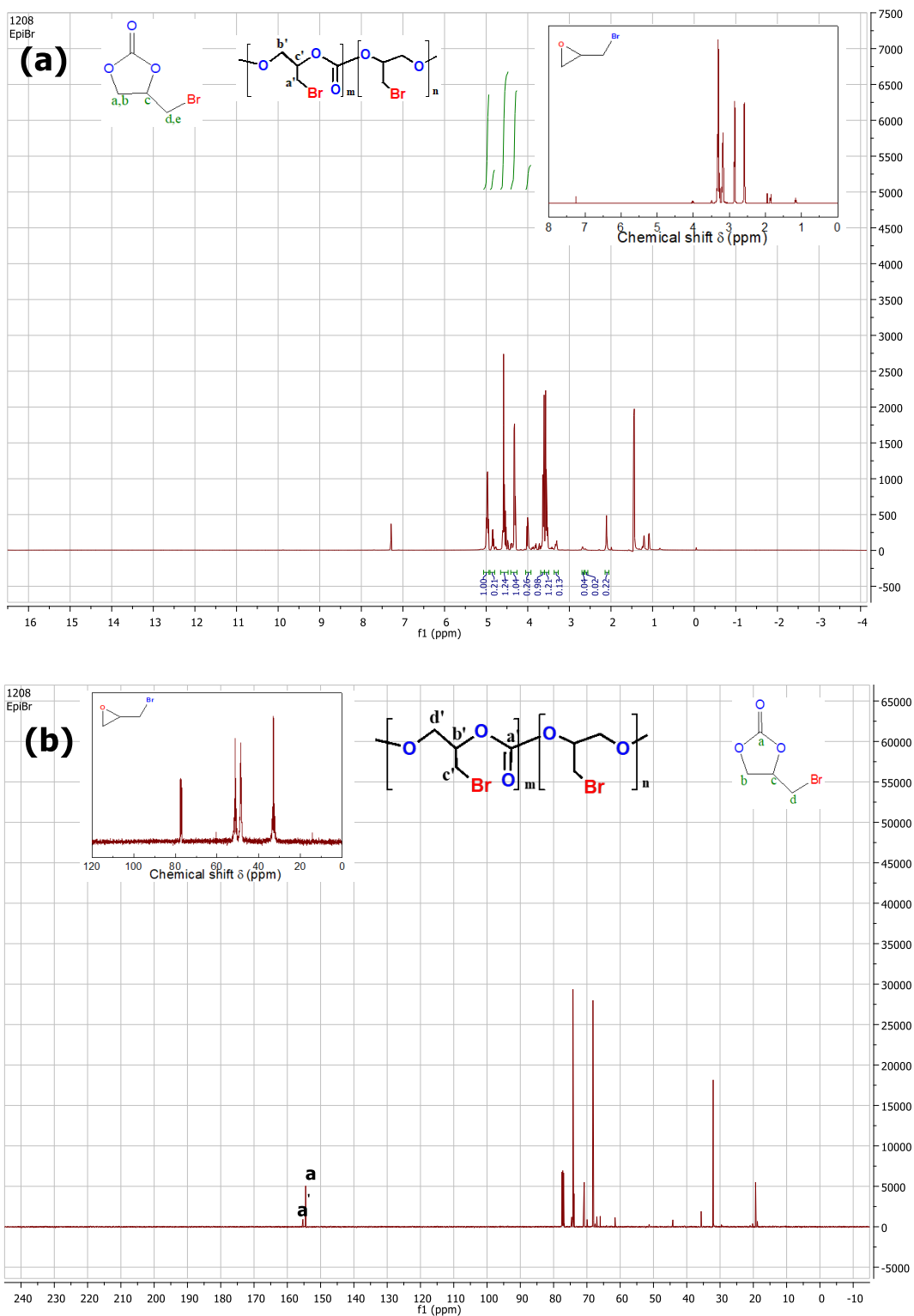


Fig. S11. (a) Crude ^1H NMR and (b) ^{13}C NMR spectrum of 4-bromomethyl-1,3-dioxolan-2-one catalysed by CHNM.

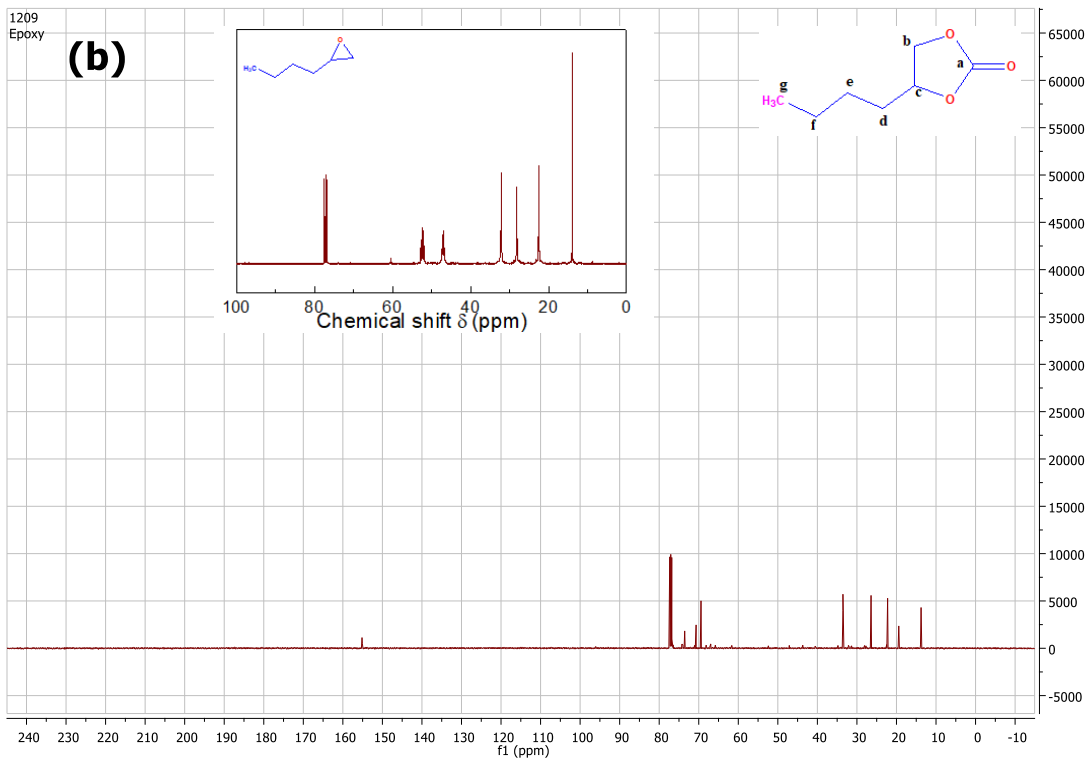
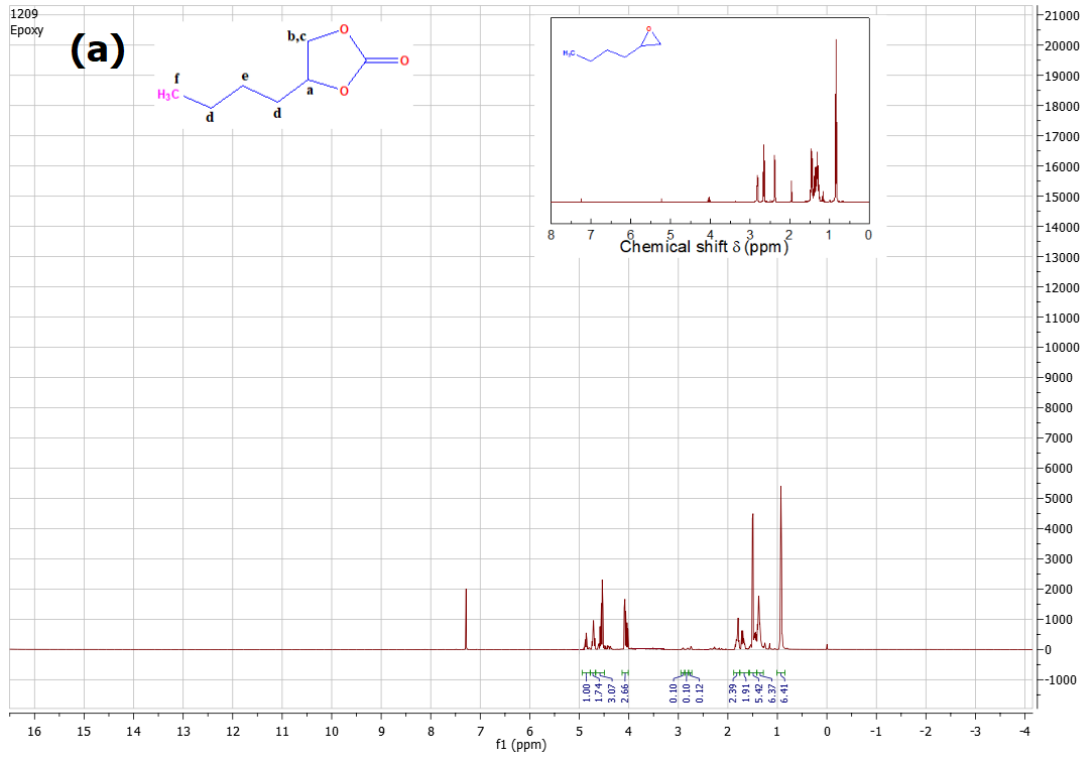


Fig. 12. (a) Crude ^1H NMR and (b) ^{13}C NMR spectrum of 4-Butyl-1,3-dioxolan-2-one catalyzed by HNM.

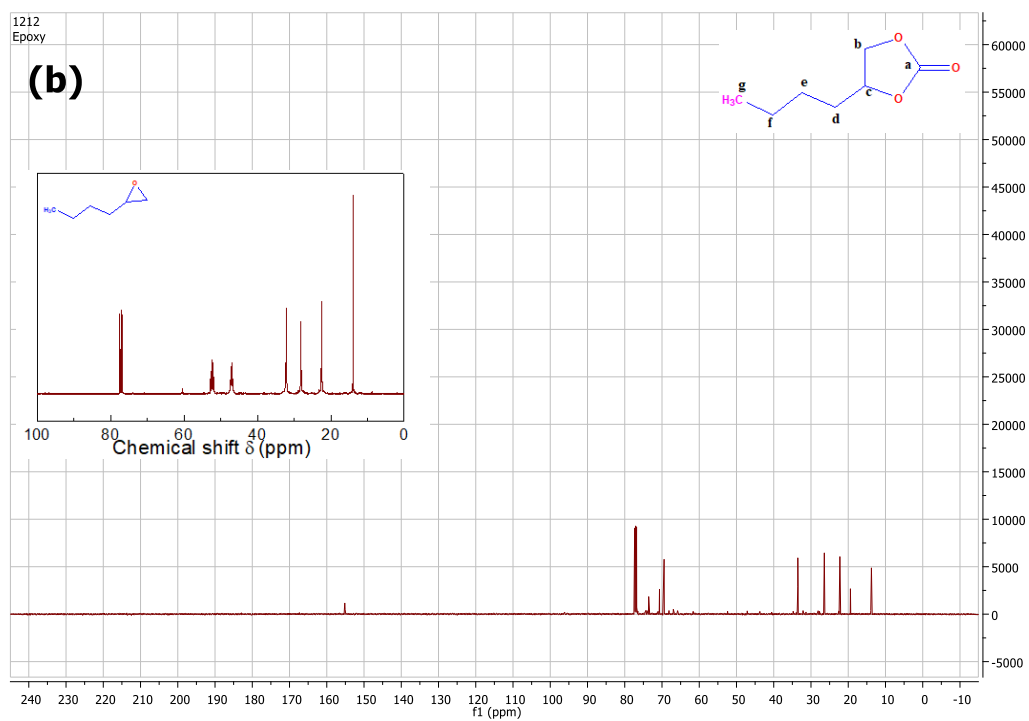
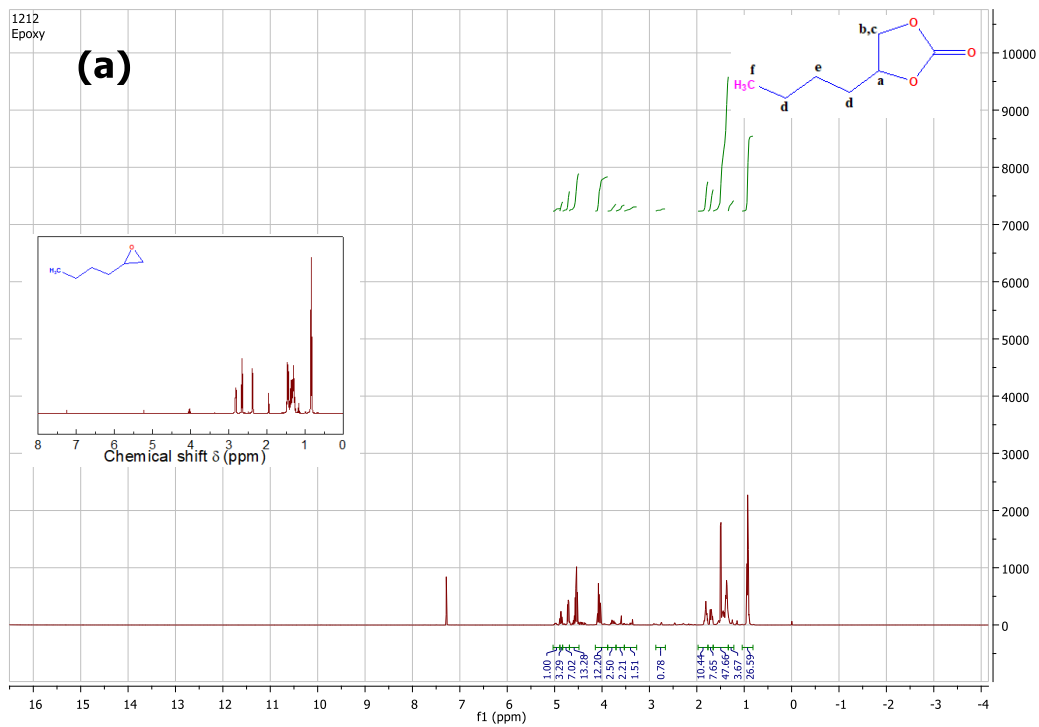


Fig. S13. (a) Crude ^1H NMR and (b) ^{13}C NMR spectrum of 4-Butyl-1,3-dioxolan-2-one catalyzed by CHNM.

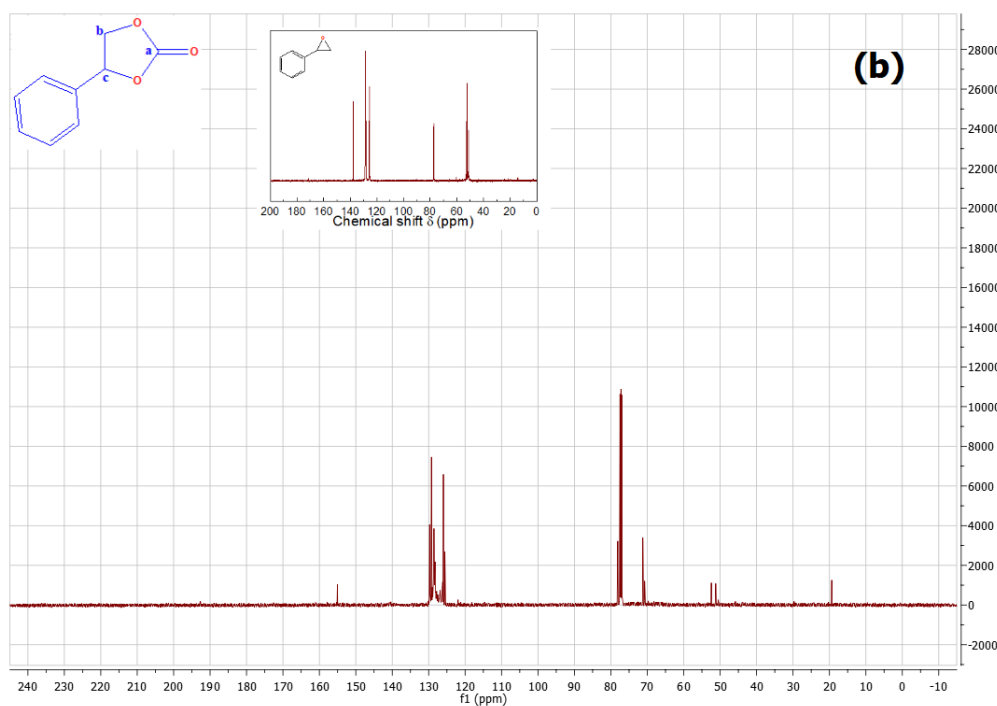
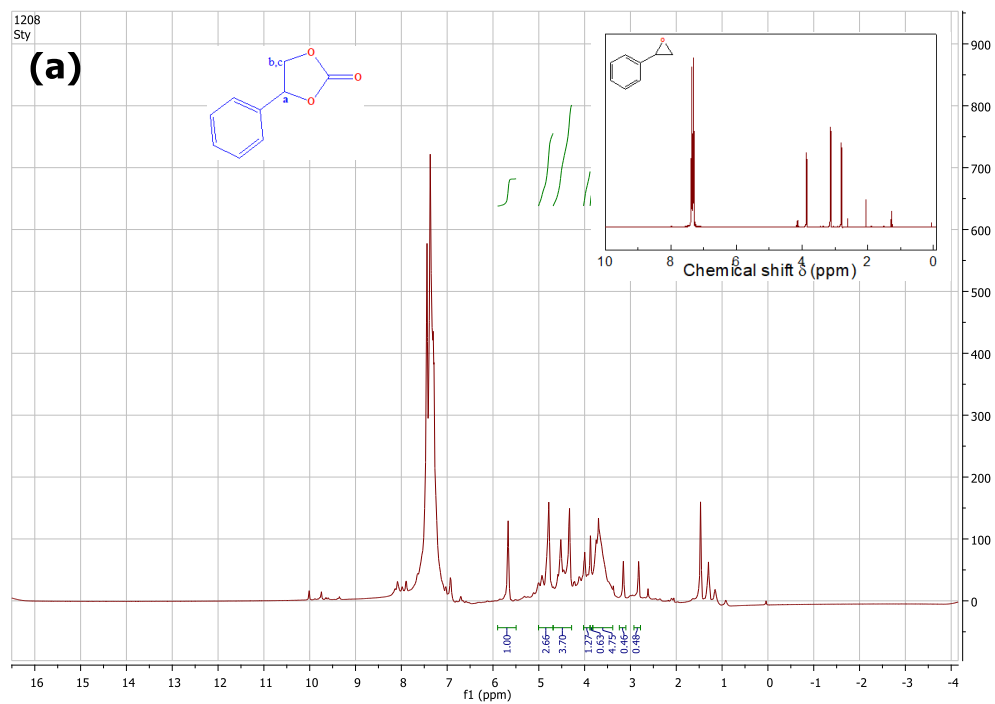


Fig. S14. (a) Crude ^1H NMR and (b) ^{13}C NMR spectrum of 4-Phenyl-1,3-dioxolan-2-one catalyzed by HNM.

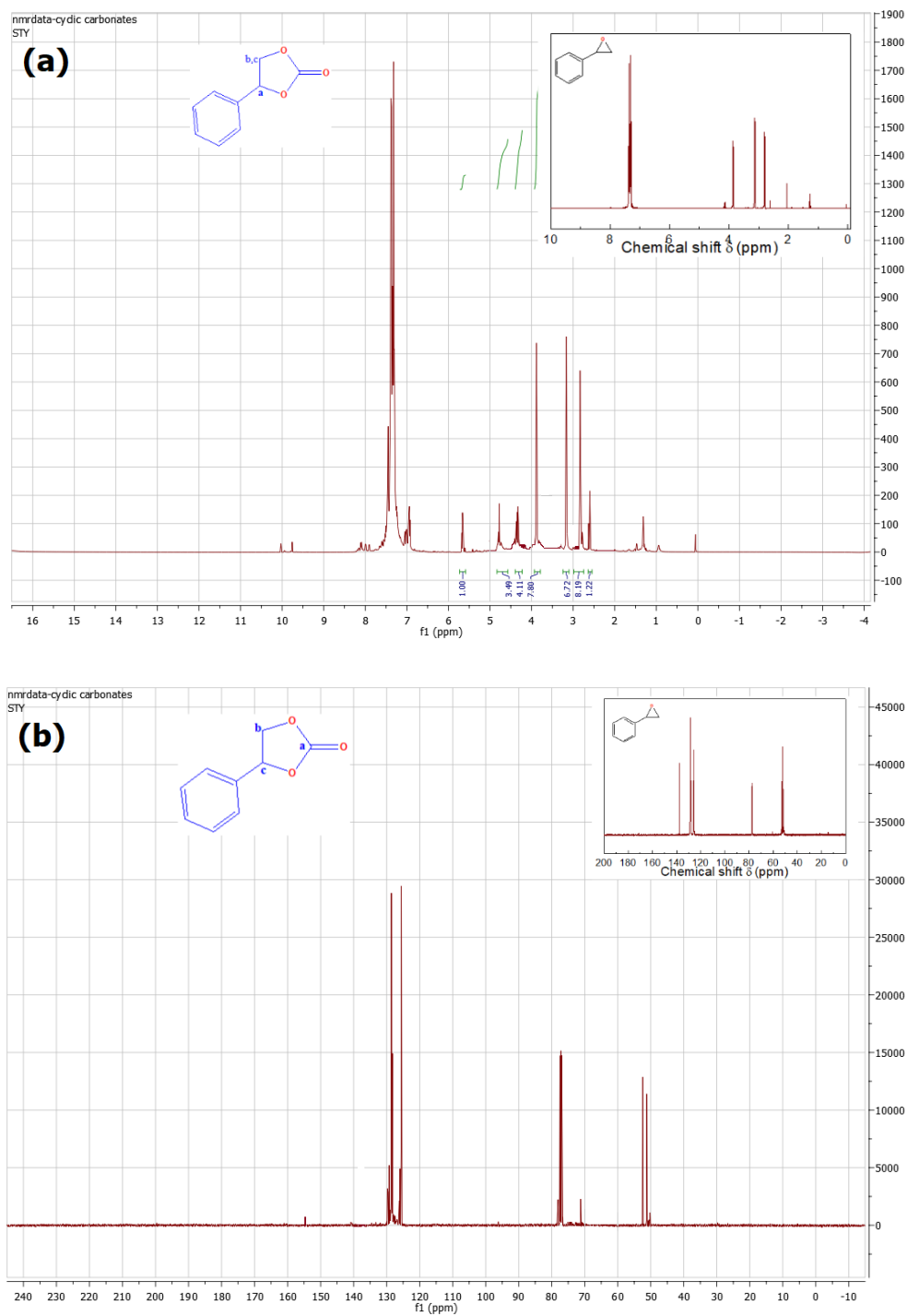


Fig. S15. (a) Crude ^1H NMR and (b) ^{13}C NMR spectrum of 4-Phenyl-1,3-dioxolan-2-one catalyzed by CHNM.

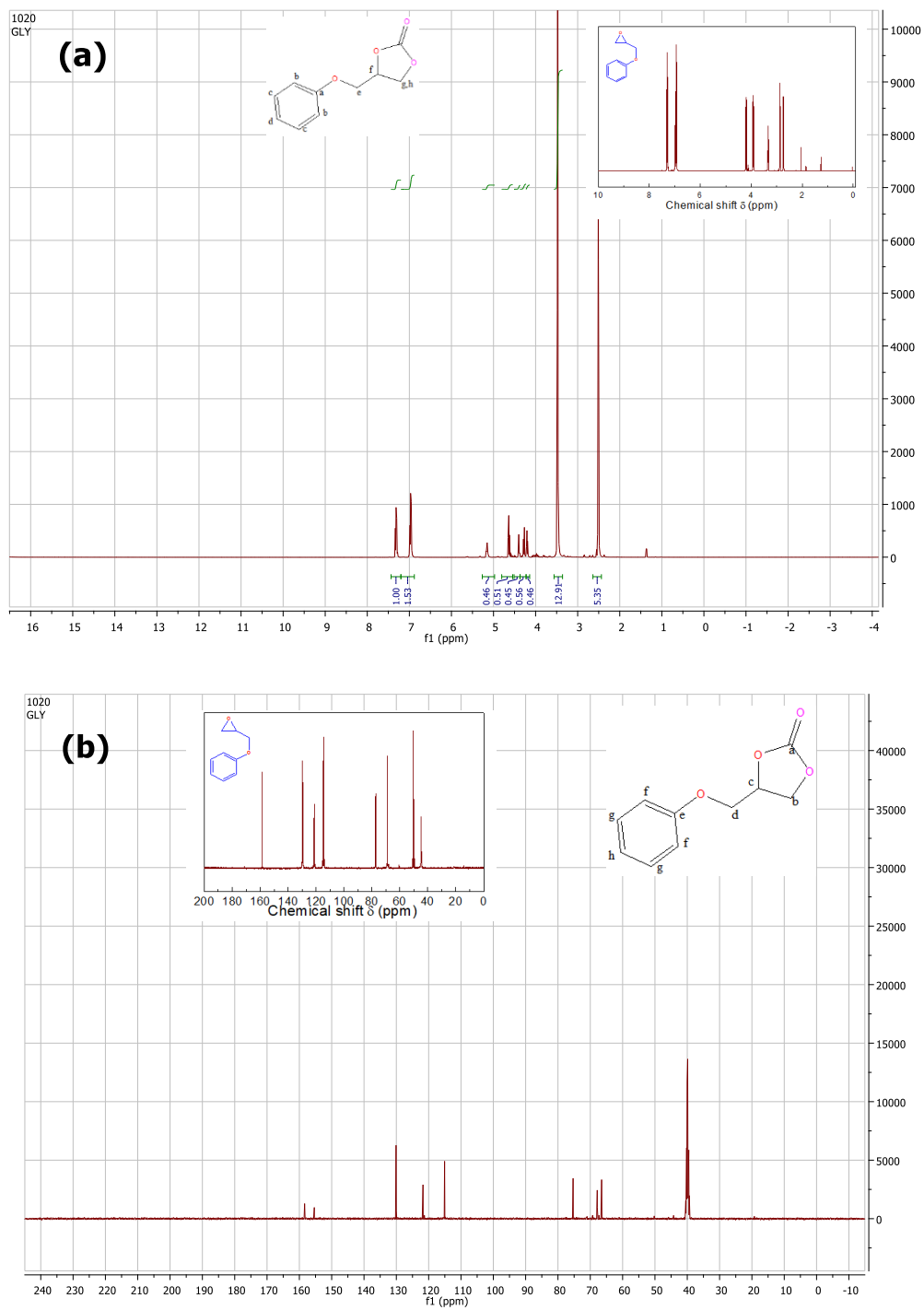


Fig. S16. (a) Crude ^1H NMR and (b) ^{13}C NMR spectrum of 4-Phenoxy methyl-1,3-dioxolan-2-one catalyzed by HNM.

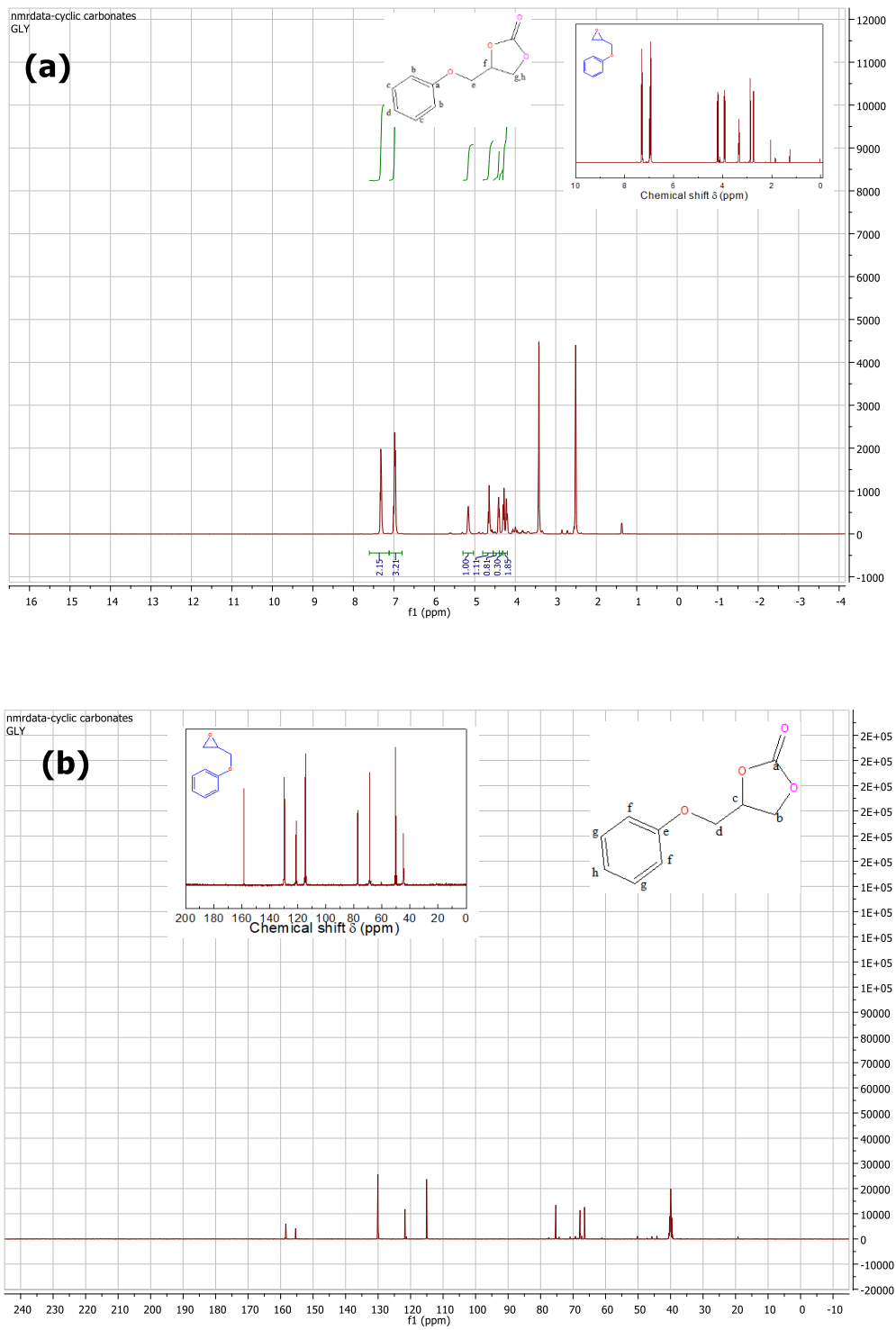


Fig. S17. (a) Crude ^1H NMR and (b) ^{13}C NMR spectrum of 4-Phenoxy methyl-1,3-dioxolan-2-one catalyzed by CHNM.

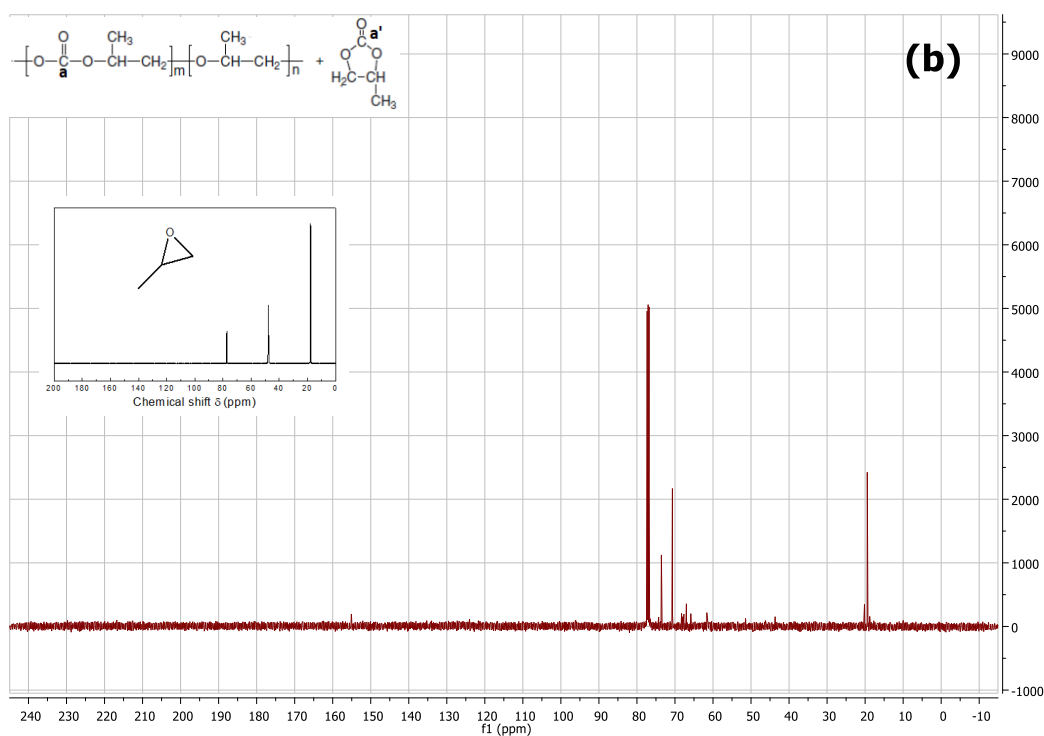
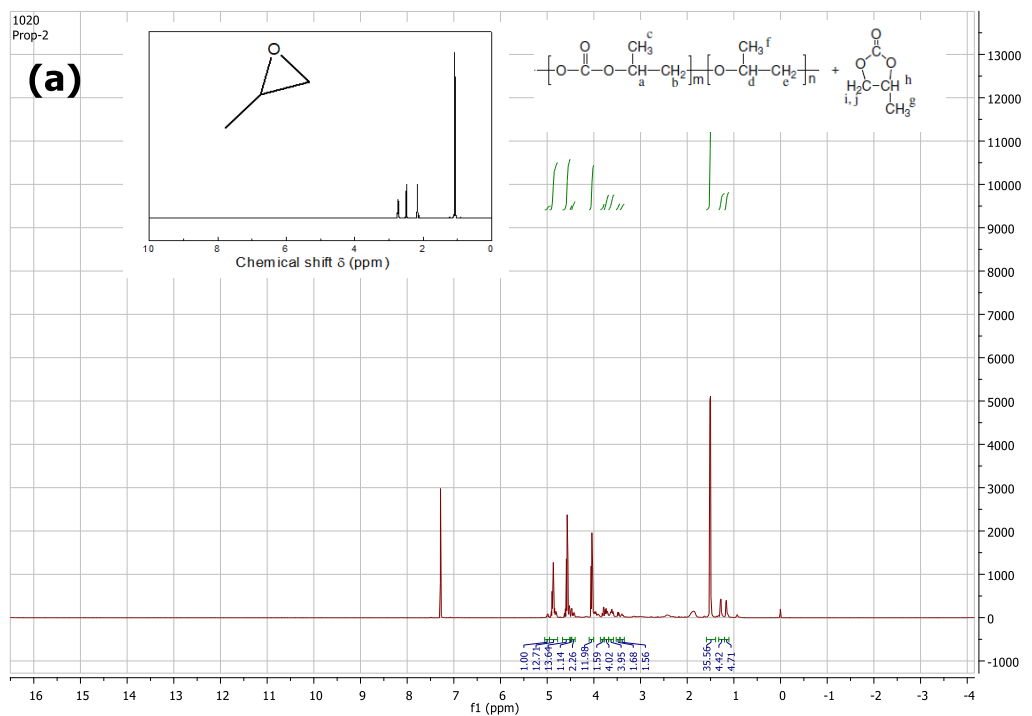


Fig. S18. (a) Crude ^1H NMR and (b) ^{13}C NMR spectrum of polypropylene carbonate and cyclic propylene carbonate catalyzed by HNM.

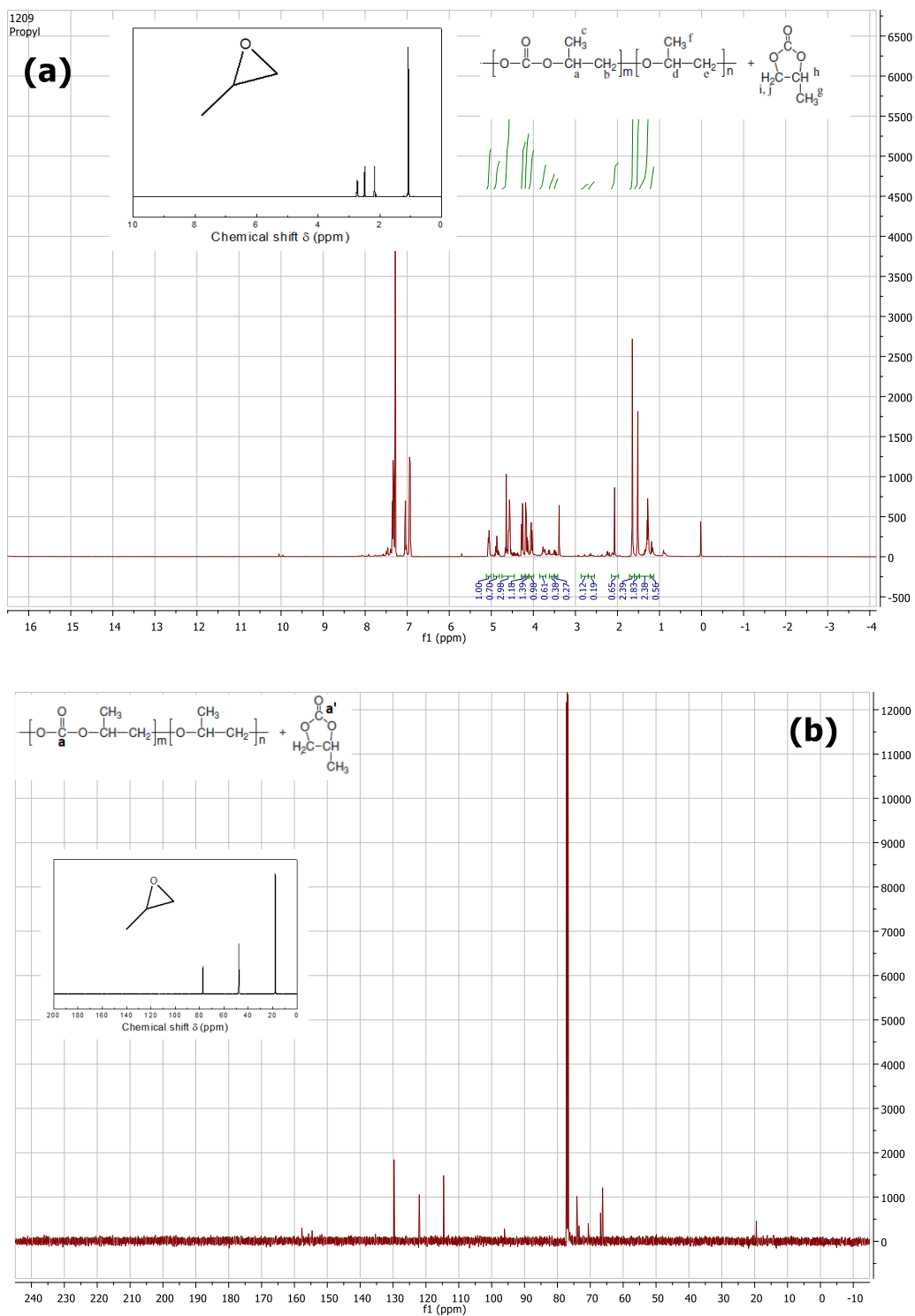


Fig. S19. (a) Crude ^1H NMR and (b) ^{13}C NMR spectrum of polypropylene carbonate and cyclic propylene carbonate catalyzed by CHNM.

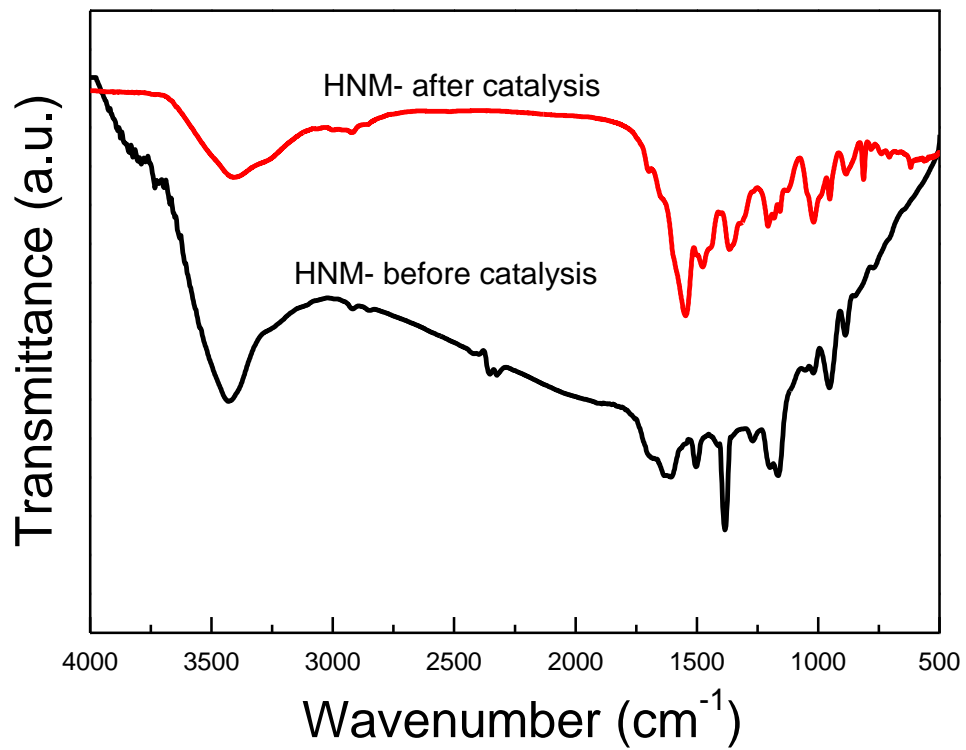


Fig. S20. FTIR spectra of HNM before and after recyclability study.

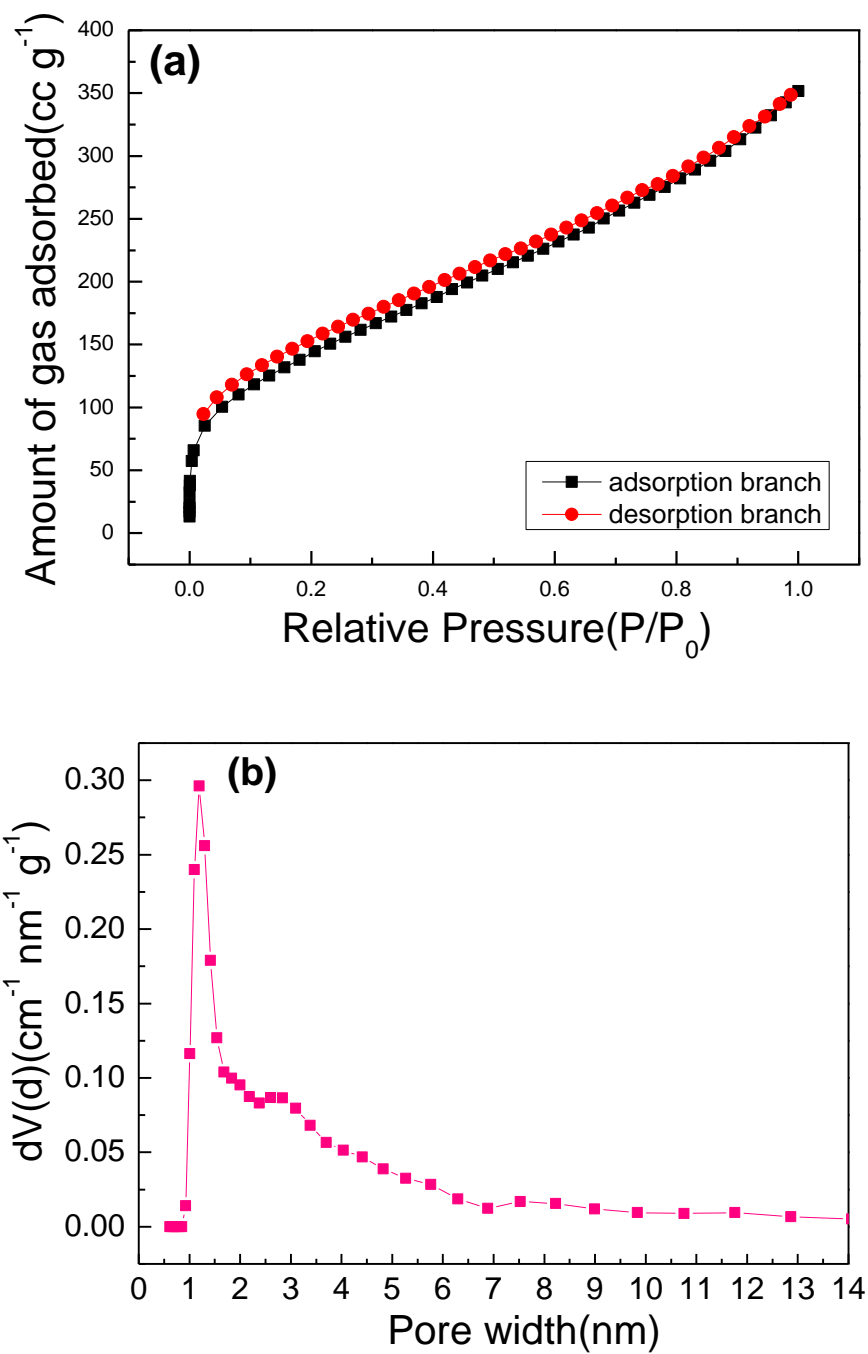


Fig. S21. (a) N₂ sorption isotherm and (b) Pore size distribution of HNM after recyclability.

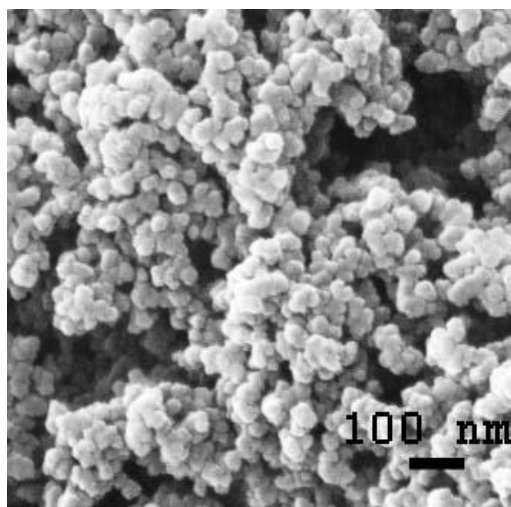


Fig. S22. FESEM image of HNM after recyclability study.

Table-S3: Current literature on CO₂ cycloaddition with epichlorohydrin over various metal free and metal-based catalysts.

S. No.	Catalysts	S _{ABET} (m ² g ⁻¹)	Epoxide	Co-catalyst	Time (h)	Temp. (°C)	pCO ₂ /bar	% Conv./Yield	Ref.
1.	IT-POP-1	245	Epichlorohydrin	-	10	120	10	99	3
2.	HB-CTP	51.2	Epichlorohydrin	TBAB	12	80	20	99	4
3.	MOSB	33.64	Epichlorohydrin	-	2	120	20	99	5
4.	cCTF-500	1247	Epichlorohydrin	-	12	90	10	95	6
5.	IPF-CSU-1	-	Epichlorohydrin	TBAB	48	25	1	95	7
6.	COF-JLU6, COF-JLU7	1450, 1392	Epichlorohydrin	TBAB	48	40	1	92	8
7.	TBICOF	1424	Epichlorohydrin	TBAB	24	26-28	1	95	9
8.	MOP-0	211	Epichlorohydrin	TBAB	24	100	10	89	10
9.	CUP	13	Propylene oxide	-	12	120	60	99	11
10.	COP-Al (metal based)	34	Epichlorohydrin	-	18	90	10	98.1	12
11.	MIL-101(Cr) (metal based)	1146	Epichlorohydrin	-	1	120	10	99.4	13
12.	POP-PBnCl-TPPMg-12 (metal based)	411	Epichlorohydrin	-	48	40	1	99	14
13.	MA500	635	Epichlorohydrin	-	15	150	15	>99	15
14.	B-SBA-15-NH ₂	250	Epichlorohydrin	KI	6	120	20	75	16
14.	HNM	807	Epichlorohydrin	-	36	100	4	100	This work

References:

1. Muhammad, R., Mohanty, P. Cyclophosphazene-based hybrid nanoporous materials as superior metal-free adsorbents for gas sorption applications. *Langmuir* **2018**, *34*, 2926-2932.
2. Muhammad, R., Rekha, P., Mohanty, P. Amino linked inorganic-organic hybrid nanoporous materials (HNMs) for CO₂ capture and H₂ storage applications. *RSC adv.* **2017**, *6*, 17100-17105.
3. Zhong, H., Su, Y., Chen, X., Li, X., Wang, R. Imidazolium-and triazine-based porous organic polymers for heterogeneous catalytic conversion of CO₂ into cyclic carbonates. *ChemSusChem* **2017**, *10*, 4855-4863.
4. Liu, A., Zhang, J. Lv, X. Novel hydrazine-bridged covalent triazine polymer for CO₂ capture and catalytic conversion. *Chinese J. Catal.* **2018**, *39*, 1320-1328.
5. Song, X., Wu, Y., Pan, D., Wei, R., Gao, L., Zhang, J., Xiao, G. Melem based multifunctional catalyst for chemical fixation of carbon dioxide into cyclic carbonate. *J. CO₂ Util.* **2018**, *24*, 287-297.
6. Buyukcakir, O., Je, S. H., Talapaneni, S. N., Kim D., Coskun, A. Charged covalent triazine frameworks for CO₂ capture and conversion, *ACS Appl. Mater. Interfaces* **2017**, *9*, 7209-7216.
7. Yu, X., Sun, J., Yuan, J., Zhang, W., Pan, C., Liu, Y., Yu, G. One-pot synthesis of an ionic porous organic framework for metal-free catalytic CO₂ fixation under ambient conditions, *Chem. Eng. J.* **2018**, *350*, 867-871.
8. Zhi, Y. F., Shao, P. P., Feng, X., Xia, H., Zhang, Y. M., Shi, Z., Mu Y., Liu, X. M., Covalent organic frameworks: efficient, metal-free, heterogeneous organocatalysts for chemical fixation of CO₂ under mild conditions, *J. Mater. Chem. A* **2018**, *6*, 374-382.
9. Das P., Mandal, S. K., In-depth experimental and computational investigations for remarkable gas/vapor sorption, selectivity, and affinity by a porous nitrogen-rich covalent organic framework, *Chem. Mater.* **2019**, *31*, 1584-1596.

10. Zhang, N., Zou, B., Yang, G. P., Yu B., Hu, C. W. Melamine-based mesoporous organic polymers as metal-free heterogeneous catalyst: Effect of hydroxyl on CO₂ capture and conversion, *J. CO₂ Util.* **2017**, *22*, 9–14.
11. Verma, S., Kumar, G., Ansari, A., Kureshy R. I., Khan, N. U. A nitrogen rich polymer as an organo-catalyst for cycloaddition of CO₂ to epoxides and its application for the synthesis of polyurethane, *Sustain. Energy Fuels* **2017**, *1*, 1620–1629.
12. Zhang, R.Y., Zhang, Y., Tong, J., Liu, L., Han, Z.B., A bifunctional cationic covalent organic polymer for cooperative conversion of CO₂ to cyclic carbonate without c-catalyst. *Catal. Letters*, **2021**, 1-9. DOI: <https://doi.org/10.1007/s10562-021-03534-7>
13. Zou, M., Dai, W., Mao, P., Li, B., Mao, J., Zhang, S., Yang, L., Luo, S., Luo, X. Zou, J. Integration of multifunctionalities on ionic liquid-anchored MIL-101 (Cr): A robust and efficient heterogeneous catalyst for conversion of CO₂ into cyclic carbonates. *Microporous and Mesoporous Mater*, **2021**, *312*, 110750.
14. Dai, Z., Tang, Y., Zhang, F., Xiong, Y., Wang, S., Sun, Q., Wang, L., Meng, X., Zhao, L., Xiao, F.S. Combination of binary active sites into heterogeneous porous polymer catalysts for efficient transformation of CO₂ under mild conditions. *Chinese J. Catal.* **2021**, *42*, 618-626.
15. Samikannu, A., Konwar, L. J., Mäki-Arvela, P., Mikkola, J.-P. Renewable N-doped active carbons as efficient catalysts for direct synthesis of cyclic carbonates from epoxides and CO₂, *Appl. Catal. B: Environmental*, **2019**, *241*, 41-51.
16. Ye, Y., Li, D., Xu, P., Sun, J. B-Doped and NH₂-functionalized SBA-15 with hydrogen bond donor groups for effective catalysis of CO₂ cycloaddition to epoxides, *Inorg. Chem. Front.*, **2020**, *7*, 3636-3645.